Soil Biology and Biochemistry 185 (2023) 109145

Contents lists available at ScienceDirect

Soil Biology and Biochemistry

journal homepage: www.elsevier.com/locate/soilbio

Thirty years of increased precipitation modifies soil organic matter fractions but not bulk soil carbon and nitrogen in a mesic grassland

Katherine S. Rocci[a,b,1,2,*], Michael Bird[c], John M. Blair[d], Alan K. Knapp[e], Chao Liang[f], M. Francesca Cotrufo[a]

[a] Soil and Crop Sciences Department, Colorado State University, Fort Collins, CO, USA
[b] Graduate Degree Program in Ecology, Colorado State University, Fort Collins, CO, USA
[c] Centre for Tropical Environmental and Sustainability Science, James Cook University, Queensland, Australia
[d] Division of Biology, Kansas State University, Manhattan, KS, USA
[e] Department of Biology, Colorado State University, Fort Collins, CO, USA
[f] Institute of Applied Ecology, Chinese Academy of Sciences, Shenyang, China

ARTICLE INFO

Keywords:
Increased precipitation
Soil organic matter
Particulate organic matter
Mineral-associated organic matter
Global change
Konza prairie

ABSTRACT

Grassland ecosystems, which are known to be sensitive to climate change, have shown minimal responses of soil carbon (C) and nitrogen (N) pools to increased moisture availability, despite moisture-induced changes in plants and soil microbes (e.g., expected drivers of soil C and N). However, it is not clear if this apparent limited response is due to an unresponsive belowground system or because alterations in multiple soil organic matter (SOM) component pools and fluxes offset each other. To investigate potential responses of C and N in SOM to decadal increases in precipitation, we sampled soils from a 30-year precipitation augmentation experiment in an annually burned mesic grassland. We measured C and N in three SOM fractions which vary in their plant and microbial controls 1) free particulate OM (fPOM), 2) occluded POM plus heavy, coarse OM (oPOM + hcOM), and 3) mineral-associated OM (MAOM), as well as amino sugars, pyrogenic C and N, and root quality metrics. We found no changes in bulk C or N under increased precipitation, but SOM fractions were modified. Altered plant inputs and soil N availability appeared to drive the responses of fPOM N and oPOM + hcOM C:N, which were increased and decreased, respectively, by increased precipitation. In contrast, the observed increase in MAOM C and N under increased precipitation could not be connected to a specific driver, suggesting additional plant, microbial, or mineral measurements may be required. Regardless, our results indicate that investigating SOM fractions may more directly connect soil C and N pools and their drivers, compared to measuring only bulk SOM. Further, our finding of greater stable OM (MAOM) under increased precipitation suggests soil C storage could provide a negative feedback to climate change with increased moisture availability, but the lack of bulk SOM response suggests that this feedback is not strong in mesic grasslands.

1. Introduction

Grassland ecosystems cover a third of the globe and are important for provisioning of food and fiber as well as for their potential to mitigate climate change, as they store a fifth of the world's C (Reynolds 2005; Dondini et al., 2023). However, provisioning services from these systems, especially ecosystem C storage, are vulnerable to changes in moisture availability expected with climate change (Knapp et al., 2017; Bai and Cotrufo, 2022). While predicted patterns of future precipitation are variable across the globe (Lee et al., 2021), greater precipitation is generally associated with higher plant productivity (e.g., aboveground C storage) in grasslands (Sala et al., 1988; Knapp et al., 2017). This is true even for mesic grasslands which, though water-limited (Knapp et al., 2001), maintain sufficient soil moisture to support growth throughout the growing season and represent almost a quarter of grassland systems (e.g., humid grasslands; White et al., 2000). Despite their aboveground responsiveness to climate variability, belowground plant and soil responses in more mesic grasslands have been limited and hard to

---

[*] Corresponding author. Present address: Institute for Arctic and Alpine Research, University of Colorado, Boulder, CO, USA.
E-mail address: katie.rocci@colorado.edu (K.S. Rocci).

[1] Present address: Institute of Arctic and Alpine Research, University of Colorado, Boulder, CO, USA.

[2] Present address: Institute for Global Change Biology, University of Michigan, Ann Arbor, MI, USA.

https://doi.org/10.1016/j.soilbio.2023.109145
Received 11 April 2023; Received in revised form 28 July 2023; Accepted 6 August 2023

anticipate, potentially because they are understudied compared to aboveground plant and biogeochemical responses (Wilcox et al., 2016; Yue et al., 2017; Vilonen et al., 2022).

Soil organic matter (SOM) is a central belowground component of grasslands, as it stores nutrients and C to be used by plants and microbes, but surprisingly, SOM has been shown to be relatively unresponsive to increased precipitation in meta-analyses (Yue et al., 2017; Rocci et al., 2021). Given the diverse processes and controls affecting SOM formation and loss, and the decadal timescale of SOM turnover (Cotrufo and Lavallee, 2022), it is not clear if limited belowground responses to changes in precipitation in mesic grasslands are evidence of an unresponsive system or a result of potentially offsetting responses of multiple SOM component pools and fluxes. Improved understanding of SOM responses to increased precipitation will be important for predicting future land biogeochemical feedbacks to climate change in mesic grasslands.

Changes in SOM in response to increased water availability are dependent on responses of plants and soil microbes. Plants generally respond more strongly to climate manipulation than do soil microbes (Yue et al., 2017), suggesting plant responses may be the dominant control on SOM responses to increased precipitation. Plants generally increase aboveground and belowground growth in response to increased precipitation, although this response is dampened, yet still positive, in wetter systems like mesic grasslands (Knapp et al., 2017; Wang et al. 2020, 2021). Plants responses to increased precipitation may also include altered tissue quality, which we define as increasing with the proportion of nitrogen (N) and water soluble and acid unhydrolyzable fibers, either directly or through plant community changes (Soong et al., 2015). While meta-analyses show greater responses of plant quality in drier sites that experience long-term or large increases in precipitation, there is mixed evidence for mesic grassland sites, with minimal response of plant tissue N but higher crude protein with higher moisture availability (Craine et al., 2010; Dumont et al., 2015; Komatsu et al., 2019; Ochoa-Hueso et al., 2020; Yue et al., 2020; Korell et al., 2021; Wu et al., 2022). Greater plant input, potentially of higher quality, may promote both SOM formation and long-term stabilization under increased precipitation, since removing plant inputs strongly reduces C content in prairie soils (Lajtha et al., 2014), and higher quality inputs can promote formation of more stable SOM (Cotrufo et al., 2013).

Although plants generally respond more strongly than soil microbes in altered precipitation experiments, microbes have evolved a number of traits to manage both deficit and excess water, as water is key for biogeochemical reactions and substrate and microbial movement (Jansson and Hofmockel, 2020). In mesic systems, increased soil moisture has the potential to push microbes past their optima and reduce their activity due to oxygen limitation (Knapp et al. 2008; Moyano et al., 2013). Thus, while soil microbial biomass generally increases with increased precipitation, there is mixed evidence (increase and neutral) in mesic systems, and little data on responses of microbial community composition in mesic grasslands (Liu et al., 2016, Zhou et al., 2018; Xu et al., 2020). Similar to microbial biomass, soil respiration responses are generally positive but only weakly positive to neutral in mesic systems, although these responses seem be driven by autotrophic respiration (e.g., plants) across aridity gradients (Liu et al., 2016; Moinet et al., 2016; Yang et al., 2020; Diao et al., 2022, Zhang et al., 2022b). Despite this, oxidative enzyme activity can be stimulated by increased precipitation in wetter ecosystems, suggesting increased microbial activity in mesic systems may be limited to decomposition of lower quality substrates (Ren et al., 2017; Jing et al., 2018). Given that both plant and microbial responses influence SOM and these drivers are rarely measured simultaneously, predicting the response of SOM to increased water availability has proven difficult.

Soil organic matter is made of a diversity of compounds. By separating SOM into constituent components, we can investigate more homogenous and discrete pools that may have relatively unique plant and microbial controls. Different SOM physical components, or fractions, have different pathways of formation and mechanisms of protection (Cotrufo and Lavallee, 2022), and respond differently to global changes and across gradients in climate (Haddix et al., 2020; Rocci et al., 2021). For example, free particulate organic matter (fPOM), which is not protected by aggregates, is most similar to plant inputs in its quality and lacks physical protection from decomposition, reducing its persistence (Six et al., 2001; Heckman et al., 2022). Under increased precipitation, increased microbial decomposition of lower quality substrates could override increased plant inputs and reduce fPOM (Ren et al., 2017; Wang et al., 2021). In contrast, occluded POM (oPOM), which is protected in aggregates and largely of plant origin, may increase with increased precipitation (Six et al., 2001). This would result from increased plant input coupled to increased aggregation with higher precipitation (Caplan et al., 2019; Bai et al., 2020; Wang et al., 2021). Mineral-associated organic matter (MAOM) is thought to form via two main pathways. These are 1) the *ex vivo* pathway, where dissolved organic matter (DOM), produced either directly (i.e., exudation and leaching) or following exoenzyme processing of structural inputs and POM, sorbs to mineral surfaces and 2) the *in vivo* pathway, where DOM substrates are taken up by microbes whose products and necromass sorb to mineral surfaces (Cotrufo et al., 2015; Liang et al., 2017). The *ex vivo* pathway may be more important in mineral-rich, microbe-poor bulk soil, while the *in vivo* pathway may dominate in high-input, microbe-rich rhizosphere (Sokol et al., 2019). Greater DOM from higher root production and turnover, and greater microbial biomass resulting from increased precipitation may spur MAOM formation via both *ex vivo* and *in vivo* pathways, respectively (Bai et al., 2010; Zhou et al., 2018; Haddix et al., 2020; Wang et al., 2021). However, little is known about the influence of increased precipitation on microbial necromass and MAOM desorption, important controls on the formation and loss of MAOM, respectively. Although, there is evidence to suggest that drying-rewetting cycles increase microbial necromass and sorption, promoting MAOM formation (Kaiser et al., 2015). These cycles could occur under increased precipitation treatments depending on the timing of increased precipitation. This potential for increased MAOM and oPOM, but decreased fPOM under increased precipitation has been supported by other studies, but the mechanisms driving these responses have not been explored (He et al., 2012; Rocci et al., 2021). Further, opposing responses of SOM fractions may explain findings of both no change and increased SOM C under increased precipitation, where differing fraction responses could be driving the overall SOM response (Yue et al., 2017; Wang et al., 2021).

The Konza Prairie Irrigation Transect Experiment has simulated increased precipitation to an annually burned tallgrass prairie by adding 29% more water on average for 30 years across a topographic gradient, providing a long-term experiment to investigate the effect of greater moisture availability on SOM, which turns over relatively slowly (Supplemental Fig. 1). Results from this experiment have revealed increases in aboveground plant growth and soil microbial activity and changes in plant community composition due to increased precipitation, depending on landscape position, but no changes in bulk soil C and N (Knapp, 1998; Wilcox et al., 2016; Broderick et al. 2022a, 2022b). Annual burning at this experiment has been suggested as a mechanism for stabilization of soil C and N pools (Wilcox et al., 2016). There has likely been increased pyrogenic (fire-altered) OM (PyOM) input in plots with increased precipitation due to increased aboveground biomass, from which PyOM originates. Increased PyOM, which is resistant to microbial decomposition, could reduce C and N losses from the soil. However, the contribution of PyOM to soil C and N pools has not yet been investigated at this site. Additionally, because bulk soil C and N integrates responses of multiple SOM fractions, the character of SOM may have changed at this site, without changes in the absolute amount of bulk soil C and N. Because fPOM, oPOM, and MAOM have different functional roles in the soil, changes in the relative distribution of C and N between these pools could modify long-term C and N stability and ecosystem functioning (Cotrufo and Lavallee, 2022).

We used this long-term irrigation experiment to determine the influence of multi-decade increased precipitation on specific SOM fractions and associated mechanisms. We tested the following three hypotheses related to influence of increased precipitation on SOM components and the moderating influence of soil properties: (1) Increased precipitation increases plant inputs and quality. This would translate to greater microbial processing of plant inputs, expected to increase microbial input to the MAOM pool. In addition, MAOM would increase through greater DOM which could be directly sorbed on minerals, and oPOM would increase through higher aggregation (Caplan et al., 2019). In contrast, fPOM would decrease due to stimulation of microbial decomposition (Broderick et al., 2022a) exceeding that of plant inputs. (2) The subsoils of increased precipitation plots will have greater accumulation of PyOM compared to control plots, due to increased PyOM movement to depth from greater leaching. Since landscape position influences soil properties, with feedbacks to SOM dynamics (Staub and Rosenzweig, 1992; Brubaker et al., 1993; Berhe and Kleber, 2013), (3) landscape position will interact with increased precipitation, resulting in larger responses in the lowland due to increased water retention and availability in the deeper soils.

2. Methods

2.1. Study site and experimental design

This study was conducted at the Irrigation Transect Experiment at Konza Prairie Biological Station (Kansas, USA, 39°09′N, 96°55′W). Konza Prairie has a mean annual temperature of 12.8 °C and mean annual precipitation of 863 mm (30-year averages). Precipitation at this site exhibits high intra- and inter-annual variability and ranges from 569 to 1674 mm per year (Supplementary Fig. 1a). The irrigation experiment is described in detail elsewhere (Knapp et al., 2001) but, briefly, the site is an annually burned native tallgrass prairie that has experienced growing season irrigation scheduled according to estimates of actual evapotranspiration (AET) and soil water availability during the growing season, with the goal of minimizing plant water limitation. Operationally, this is carried out by modeling daily estimated plant AET (Moore, 2023) and conducting periodic measurements of soil water content to assess irrigation timing and amounts required to return soil water content at 0.25 $cm^3\ cm^{-3}$ or higher to 30 cm depth (Knapp et al., 2001). This causes the magnitude of water addition to vary year-to-year but has resulted in a 29% increase in annual precipitation on average which also has slightly decreased interannual variability (Supplementary Fig. 1a). This water addition increased soil moisture by 4.5% on average for years with comparable data (2006–2009, 2013, 2017–2021), although this is highly variable within and among years, and also slightly decreased intra-annual variability (Supplementary Fig. 1b). We focus on average precipitation and soil moisture increases because we are largely investigating slow-turnover pools that we expect to be minimally affected by climate at the time of sampling (Delgado-Baquerizo et al. 2017a, 2017b). The experiment transect spans a topographic gradient, with the upland soils classified as fine, mixed mesic Udic Haplustolls (0–10 cm: 15% sand, 58% silt, 27% clay) and the lowland soils classified as fine, mixed Pachic Argiustolls (0–10 cm: 15% sand, 51% silt, 34% clay; Broderick et al., 2022a). The site is dominated by perennial grasses, primarily *Andropogon gerardii*, *Soghastrum nutans*, *Schizachyrium scoparium,* and *Panicum virgatum*. The site has two irrigation transects, initiated in 1991 and 1993, respectively, and two non-irrigated control transects (Supplementary Fig. 2). From here forward, we refer to the irrigated treatment as the increased precipitation treatment. For each transect (2 each in the upland and lowland), each treatment (control *versus* increased precipitation) is replicated 3 times, providing a total of 24 plots (2 landscape positions x 2 treatments x 2 transects x 3 replicates).

2.2. Sampling

In September 2021, we performed soil coring at each plot. We took 4 cores per plot using a 5.25 cm diameter push corer to 30 cm, where soil depth allowed, since some upland plots had shallower soil profiles. In the field, we separated each core into three depth increments: 0–5 cm, 5–15 cm, and 15–30 cm, and bulked the 4 cores, maintaining each depth increment. This provided 72 individual observations ($n = 24$ plots × 3 depths). Soils were then transported to Colorado State University in coolers for subsequent analyses.

2.3. Soil analyses

All soil samples were sieved though 8 mm mesh and a subsample was subsequently sieved through 2 mm mesh. We collected roots and coarse material (aboveground plant material and rocks) during sieving and used the weight of these and the soil to calculate bulk density and to determine root biomass distribution (Mosier et al., 2021). For root biomass, we only report coarse roots (from 8 mm sieving) since they were the dominant root mass in the soil and roots from 2 mm sieving were unaffected by treatment or landscape position. We used air-dried 2 mm sieved soil to perform a combined density and size fractionation following Haddix et al. (2020), on the 0–5 cm and 5–15 cm depth soils ($n = 48$). We found relatively small responses of SOM fraction C and N for these initial depths (Fig. 1) and were limited by shallow upland soils, so we did not fractionate the 15–30 cm depth soils. Briefly, 10.5 g of soil was shaken with deionized water and then centrifuged and filtered through a 20 μm nylon filter to retrieve the DOM pool. The soil was then centrifuged with sodium polytungstate at a density of 1.85 $g\ cm^{-3}$ to separate the light and heavy fractions of SOM. The light, floating, fraction was aspirated as free POM (fPOM). The remaining soil (the heavy fraction) was then dispersed using 0.5% sodium hexametaphosphate and 12 glass beads. After shaking for 18 h, the slurry was poured over a 53 μm sieve, with the fraction passing through designated as MAOM and the fraction >53 μm designated as occluded POM and heavy, coarse OM (oPOM + hcOM; *sensu* Leuthold et al., 2022). Each fraction was subsequently weighed to determine recovery, which was 98.3% on average and varied from 94.6 to 102.7%. Concentrations of C and N in SOM, fPOM, oPOM + hcOM, and MAOM were measured on a VELP 802 elemental analyzer (VELP Scientific, Inc., Long Island, New York). Concentrations of C and N in DOM were measured on a Shimadzu TOC-L (Shimadzu Scientific Instruments, Inc., Columbia, Maryland).

We measured amino sugars in the bulk soil as a proxy for microbial necromass, which is thought to be a precursor for MAOM formation (Liang et al., 2017). We performed amino sugar measurement on the 0–5 cm and 5–15 cm depth samples, as with the fractionation, and limited this analysis to the lowland soils ($n = 24$) because they appeared to be more responsive than upland soils to the increased precipitation treatment. We followed the procedure of Zhang and Amelung (1996) to determine the amount of muramic acid (MurA), glucosamine (GluN), and galactosamine (GalN). Briefly, the soils were acid digested for breaking up amino sugar polymers, then the three amino sugar monomers were purified, and derivatized for measurement. For acid hydrolysis, dry soils containing approximately 0.3 mg N were mixed with 6 M HCl at 105 °C for 8 h. The hydrolysates then underwent several purification steps. First, samples were filtered through 55 mm glass fiber filters and evaporated to dryness on a rotary evaporator at 52 °C under vacuum. Residues were then dissolved in deionized water (DI) and brought to a neutral pH before centrifugation to remove salts. The supernatant was then freeze-dried, resuspended in methanol, dried using N_2 gas at 45 °C, re-dissolved in 1 ml DI, and lyophilized. For derivatization, the sample was heated with a reagent (hydroxylamine hydrochloride and 4-(dimathylamino) pyridine in pyridine-methanol) and then with acetic anhydrite at 75–80 °C. Dichloromethane was then added to the sample and excess reagent was removed following washing with HCl and DI. The sample was then dried and resuspended in ethyl

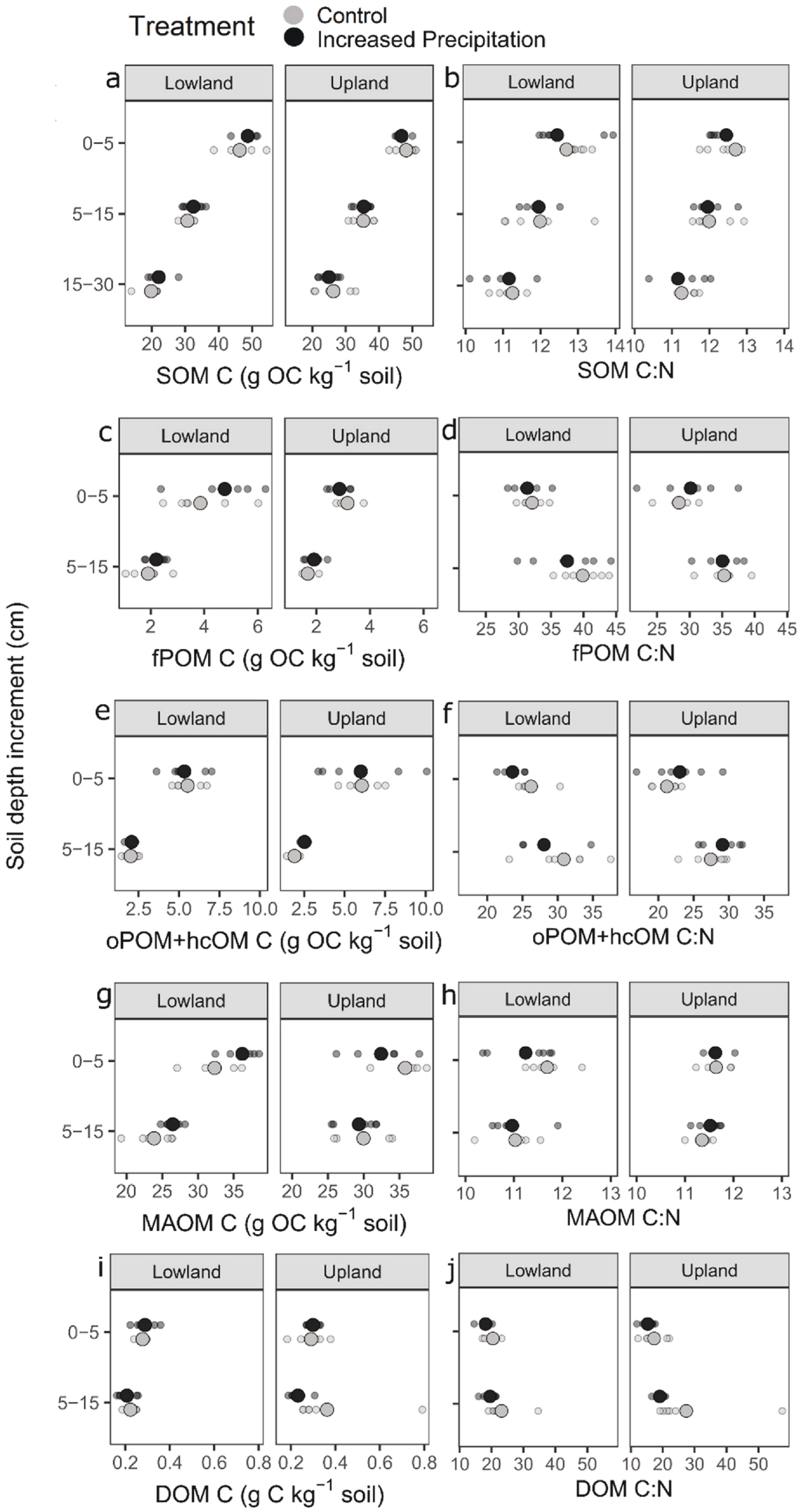

Fig. 1. Soil organic matter (SOM) carbon (C) and carbon-to-nitrogen ratio (C:N; a, b), free particulate OM (fPOM) C and C:N (c, d), occluded POM and heavy, coarse OM (oPOM + hcOM) C and C:N (e, f), mineral-associated OM (MAOM) C and C:N (g, h), and dissolved OM (DOM) C and C:N (i, j) in response to increased precipitation (black) *versus* a control (gray) across soil depths and landscape positions. Large circles are mean values and small circles below are individual observations (n = 6).

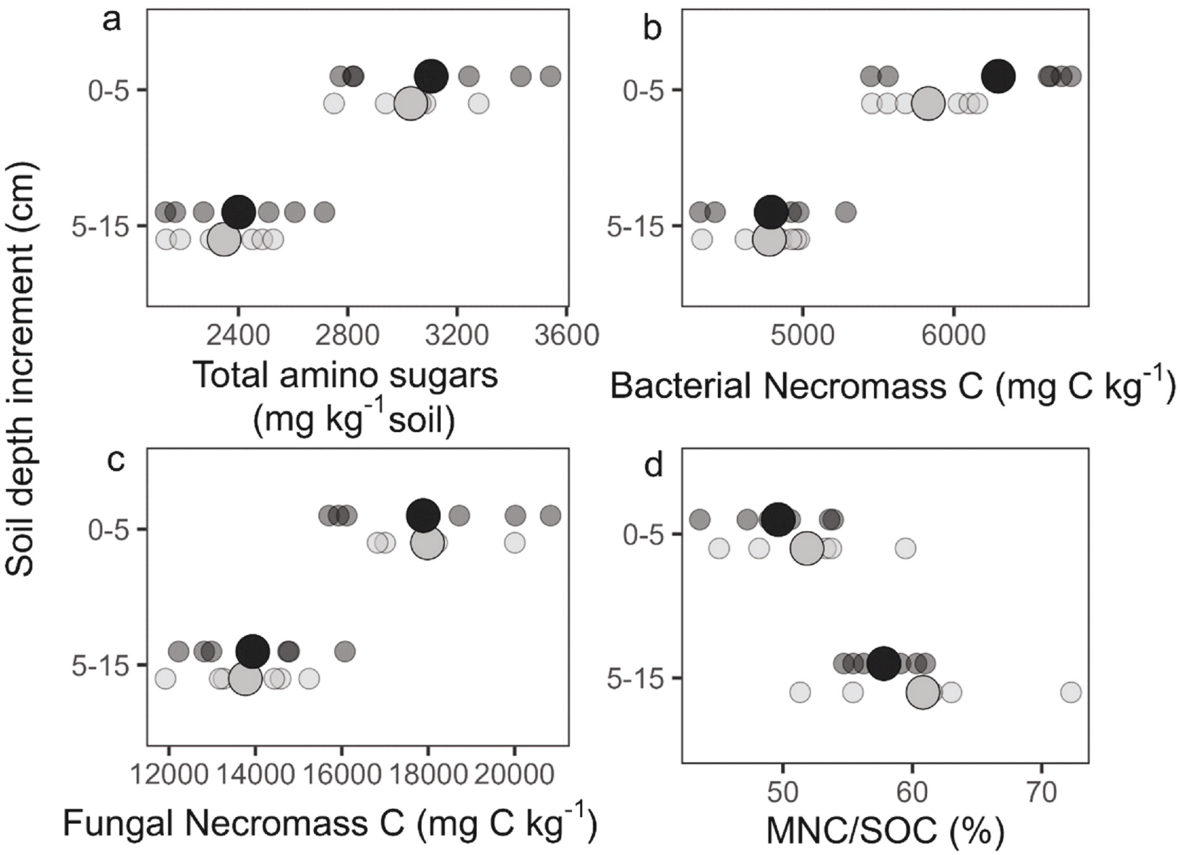

Fig. 2. Total amino sugars (a), bacterial necromass carbon (b), fungal necromass carbon (c), and percent of microbial necromass carbon of soil organic carbon (MNC/SOC; d) in response to increased precipitation (black) *versus* a control (gray) across soil depths for the lowland soils only. Large circles are mean values and small circles below are individual observations (n = 6).

acetate-hexane (1:1) for measurement. Samples were analyzed on an Agilent 7890B GC (Agilent Technologies, Santa Clara, CA, USA) that was equipped with a HP-5 column (30 m length × 0.25 mm diameter × 0.25 μm thickness) and flame ionization detector. Myo-inositol and methylglucamine were used as an internal standard and recovery standard. The contents of individual amino sugars were calculated based on the internal standard. Total amino sugars were determined as the sum of MurA, GluN, and GalN. Total microbial necromass C was calculated at the sum of bacterial and fungal necromass C. For bacterial necromass C, we converted MurA using a conversion factor of 45, and for fungal necromass C, we subtracted out bacterial content of GluN and converted corrected GluN using a conversion factor of 9 (Joergensen 2018; Liang et al., 2019):

$$\text{Bacterial necromass C} = \text{MurA} * 45 \tag{1}$$

$$\text{Fungal necromass C} = \left(\frac{\text{GluN}}{179.17} - \left(2*\frac{\text{MurA}}{253.23}\right)\right) \times 179.17 \times 9 \tag{2}$$

We estimated pyrogenic C and N (PyC and PyN) using hydrogen pyrolysis (Wurster et al., 2012; McBeath et al., 2015). Subsamples of 250 mg of soil were combined with an amount of molybdenum catalyst approximately equal to 1% of soil organic C for each subsample. This was done using an aqueous/methanol solution of ammonium dioxydithiomolybdate. The dried, catalyst-loaded subsamples were pressurized with 15 MPa of hydrogen with a sweep gas flow of 5 L min^{-1} in the hydrogen pyrolysis reactor (Strata Technology Ltd., Middlesex, UK). The temperature was ramped to 250 °C at a rate of 300 °C min^{-1}, then at 8 °C min^{-1} to a final temperature of 550 °C, which was held for 5 min. Following hydrogen pyrolysis, the remaining material was weighed and C and N abundance was determined on a Costech elemental analyzer (Costech Analytical Technologies, Inc., Valencia, CA) that was cross-checked to the VELP elemental analyzer (above) to ensure values were comparable. Post-hydrogen pyrolysis C and N were corrected for the amount of C and N loaded into the reactor.

2.4. *Root quality analyses*

In addition to soil analyses, we also analyzed root quality. We focused on roots, rather than aboveground material, because this site is annually burned and so roots are the more quantitatively important form of unburned plant inputs that would influence SOM in this system. All root analyses were performed on coarse roots (collected during 8 mm sieving) and root material from 5-15 and 15–30 cm depths were combined to ensure sufficient material for the analyses. We determined acid unhydrolyzable residue (AUR) and cellulose contents in the roots using the ANKOM Acid Detergent Fiber and Acid Detergent Lignin methods (ANKOM Technology 2022). Briefly, 0.45–0.55 g of ground root material were measured into 25 μm porosity filter bags (F57 filter bag, ANKOM Technology, Macedon, NY). Filter bags were placed in an ANKOM A200 (ANKOM Technology, Macedon, NY) and agitated for 1 h in acid detergent solution containing 93.2% water, 4.8% sulfuric acid, and 2% cetyltrimethylammonium bromide (Midland Scientific, Inc., Omaha, NE). Bags were then rinsed with deionized water and dried to 105 °C and weighed to determine acid detergent fiber (W1). Dried bags were then submerged in H_2SO_4 for 3 h and agitated every 30 min to remove cellulose. They were then rinsed with deionized water until the pH was neutral and then dried to 105 °C and weighed to determine AUR + ash (W2). Bags were then ashed in a muffle furnace at 525 °C for 3 h to remove AUR and weighed to determine residual ash (W3). Cellulose and AUR were determined as the difference between W1 and W2 and W2 and

W3, respectively. Two filter bags (an upland and lowland increased precipitation replicate) opened during this procedure and, because we did not have enough root material to repeat the procedure, these were removed from analysis (below).

We also analyzed the amount of hot water extractable (HWE) material in the roots using the method by Tappi (1981), as modified by Soong et al. (2015). Since HWE-C is highly correlated with leaching of dissolved organic C during early phases of plant decomposition, we use it as a proxy for readily available plant compounds (Soong et al., 2015). We digested 0.35 g of root material cut into 1 cm pieces with deionized water at 100 °C for 3 h. We then filtered the mixture through a 20 μm nylon mesh to obtain HWE (<20 μm) and the hot water residue (>20 μm). The HWE was then frozen until being run on a Shimadzu TOC-L (Shimadzu Scientific Instruments, Inc., Columbia, Maryland) to obtain HWE-C and HWE-N.

2.5. Data analyses

Response variables for this study were C and N in SOM, DOM, oPOM + hcOM, MAOM, and root HWE, as well as root biomass, AUR, and cellulose, total amino sugars, bacterial and fungal necromass C, PyC, PyN, PyC:PyN, and the proportions of microbial necromass C and PyC and PyN in SOM-C and -N, respectively. We followed the data exploration procedures outlined in Zuur et al. (2010). We log transformed root biomass, bulk density, and a number of C and N measurements (SOM C and N stocks and C:N, oPOM + hcOM C and N stocks, MAOM C stock and C:N, PyN, PyC/SOM-C, PyN/SOM-N as well as C and N concentrations in fPOM, oPOM + hcOM, DOM, and HWE) to mitigate influential outliers or unequal variance.

We investigated whether increased precipitation modified the response variables by building random effect models with treatment, landscape position, soil depth, and their interactions as predictors and land position nested within transect as the random variable, effectively creating four blocks. Soil depth was removed as a main effect in models for C and N stocks and root biomass because soil depth segments were uneven (e.g., 5 cm, 10 cm, and 15 cm), which would lead to higher C and N stocks and root biomass in larger depth segments by default. Interactions with treatment and landscape position were retained to investigate whether treatment or landscape position effects differed within a given depth segment (e.g., increased precipitation increased MAOM C stock only in the 0–5 cm depth). Bulk density was influenced by treatment (Supplementary Table 1), so SOM, MAOM, fPOM, and oPOM + hcOM C and N stocks were analyzed using an equivalent soil mass approach with the control soils as the reference mass (Ferchaud and Chlebowski, 2020). To investigate the influence of soil depth, we determined response of soil C and N concentrations as well as stocks.

To investigate the relationships between SOM fraction C and N and plant and microbial drivers, we created multiple regression models with standardized (mean = 0 and standard deviation = 1) predictors separately for the upland and lowland sites, due to different number of predictors for each landscape position. To reduce the number of predictors we used the first axis of a principal components analysis (PC1) on the root quality data (root AUR, cellulose, and HWE C and N) which explained 44% of the variance and was associated with lower plant quality, as it was positively associated with AUR (eigenvector = 0.51) and negatively associated with HWE C and N (eigenvectors = −0.52 and −0.66, respectively). For upland sites, we used the root quality PC1, root biomass, and their interactions with treatment as predictors for all fractions. We added DOM and its interaction with treatment to the MAOM model, given the expectation that DOM is a precursor for MAOM formation (Cotrufo et al., 2015). Lowland models were the same as upland models except that total amino sugars and its interaction with treatment were added to all models, given the expectation that microbial residues can contribute to SOM fractions (Cotrufo and Lavallee, 2022). Statistical analyses were carried out in RStudio v4.0.2 (R Core Team 2019) with significance determined at $p < 0.05$.

3. Results

3.1. Soil organic matter carbon and nitrogen

The concentrations of C and N in bulk SOM were not responsive to the increased precipitation treatment, but C and N concentrations in specific SOM fractions were (Fig. 1; Supplementary Table 2). The concentration of N in fPOM was 8% higher under increased precipitation compared to control plots ($p = 0.045$; Supplementary Fig. 3). Additionally, C and N concentrations in MAOM were 7 and 9% higher, and the C:N ratio of oPOM + hcOM was 7% lower under increased precipitation compared to the control plots, but only in the lowland (all $p < 0.05$; Fig. 1; Supplementary Fig. 3; Supplementary Table 2). In contrast, DOM C concentration was 18% higher under control than increased precipitation treatments in the 5–15 cm depth ($p = 0.007$). This drove 13% higher DOM C:N in the control compared to the increased precipitation treatment ($p = 0.022$; Fig. 1). The interaction of landscape position and soil depth was also significant for bulk SOM C concentrations and C:N and MAOM C and N concentrations (Supplementary Table 2; Supplementary Fig. 3; Fig. 1). Bulk SOM C and MAOM C and N concentrations were higher in the upland than lowland in 5–15 cm depth (all $p < 0.05$) and SOM C:N was higher in lowland than upland plots in the 0–5 cm depth ($p = 0.031$; Fig. 1; Supplementary Fig. 3). Soil depth was a significant predictor of all SOM C and N concentrations and stoichiometries. All SOM metrics had higher values for the 0–5 cm depth, except for fPOM, oPOM + hcOM, and DOM C:N, which were higher in 5–15 cm depth (Fig. 1; Supplementary Table 2; Supplementary Fig. 3).

Soil C and N stock responses to increased precipitation were similar to those of C and N concentrations. Bulk soil C and N stocks for 0–30 cm were similar between the increased precipitation treatment and control plots, with an average of 9019 *versus* 9144 g C m^{-2} and 774 *versus* 775 g N m^{-2}, respectively. The majority of C and N was found in MAOM and fractions were more responsive to the increased precipitation treatment than were the bulk SOM C and N stocks (Supplementary Fig. 4; Supplementary Table 3). Individually, the increased precipitation treatment only influenced the fPOM N stock, increasing it by 9% compared to the control. Both MAOM C and N stocks increased under increased precipitation by 7 and 8% respectively, but only in the lowland (both $p < 0.008$; Supplementary Table 3). We also observed a marginally significant 10% increase in oPOM + hcOM-C under increased precipitation, but only for the 5–15 cm depth ($p = 0.051$; Supplementary Table 3). The C and N stocks in SOM and MAOM varied with landscape position, depending on soil depth, such that upland SOM and MAOM C and N stocks were higher than in the lowland in the 5–15 cm depth, and in the 15–30 cm depth for SOM (Supplementary Table 3). While the interaction of landscape position and soil depth was also a significant predictor of fPOM C and N stocks and oPOM N stocks, there were no significant pairwise differences between those values in the upland and lowland at any depth (Supplementary Table 3; Supplementary Fig. 4).

3.2. Amino sugars

No measure of amino sugars in the lowland soils was modified by the increased precipitation treatment (Supplementary Table 4). Total amino sugars, bacterial and fungal necromass C, and the proportion of microbial necromass C in SOM-C were all modified by soil depth, with total amino sugars and bacterial and fungal necromass C all decreasing with depth and the proportion of microbial necromass C in SOM-C increasing with depth (all $p < 0.001$, Fig. 2; Supplementary Table 4). There were no other significant predictors of any measure of amino sugars.

3.3. Pyrogenic organic matter

The ratio of PyC to PyN (PyC:PyN) was the only pyrogenic OM metric that was modified by the treatment - increased precipitation marginally increased PyC:PyN but only in the lowland ($p = 0.076$; Fig. 3; Supplementary Table 5). All measures of pyrogenic OM were modified by soil depth, where PyC and PyC:PyN decreased and PyN, PyC/SOM-C, and PyN/TN all increased with depth (Fig. 3; Supplementary Table 5). There were no other significant predictors of any measure of pyrogenic OM (Supplementary Table 5).

3.4. *Root biomass and quality*

Root biomass increased by 26% with increased precipitation, averaged across landscape position and soil depth ($p = 0.001$; Fig. 4). Root biomass also was significantly higher in the lowland than upland but only in the 0–5 cm depth ($p = 0.039$). No other pairwise comparisons were significant for root biomass (Fig. 4; Supplementary Table 6). Root AUR increased by 11% with increased precipitation in the lowland ($p = 0.010$) but was otherwise unaffected by predictor variables (Supplementary Table 6). Root cellulose was influenced by soil depth ($p = 0.011$) and its interaction with landscape position ($p = 0.024$), such that there was 12% more cellulose in roots in the 5–30 cm compared to the 0–5 cm depth in the upland. Root HWE %C, %N, and C:N were unaffected by any predictor variables (Supplementary Table 6).

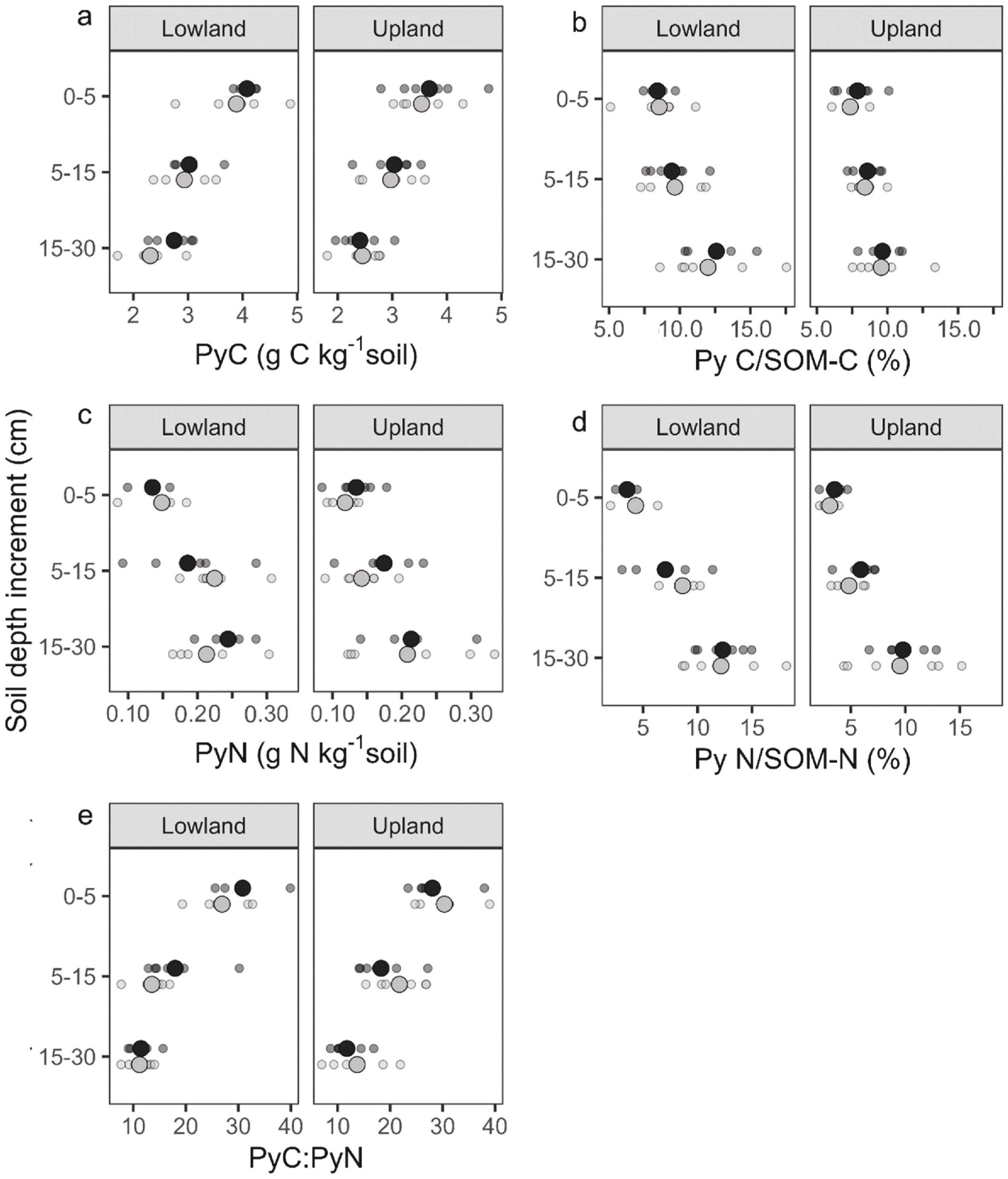

Fig. 3. Pyrogenic carbon (PyC; a), percent of soil organic matter C (SOM-C) that is PyC (b), pyrogenic nitrogen (PyN; c), percent of soil organic matter N (SOM-N) that is PyN (d), and the ratio of PyC to PyN (PyC:PyN; e) in response to increased precipitation (black) *versus* a control (gray) across soil depths and landscape positions. Large circles are mean values and small circles below are individual observations ($n = 6$).

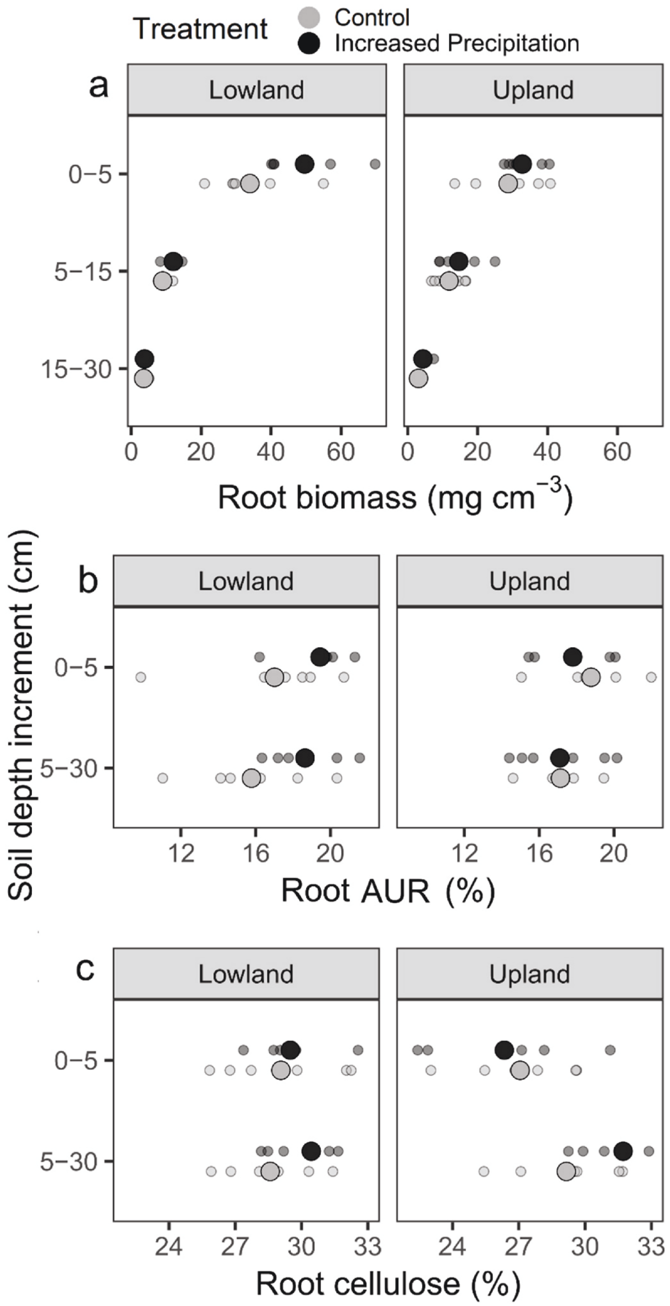

Fig. 4. Root biomass (a), acid unhydrolyzable residue (AUR; b), and cellulose (c) in response to increased precipitation (black) *versus* a control (gray) across soil depths and landscape positions. Large circles are mean values and small circles below are individual observations ($n = 6$).

3.5. Multiple regression

When combining plant and microbial drivers into models for SOM fractions, we found unique associations for each fraction, but very similar responses of C and N for a given fraction (Fig. 5). In both uplands and lowlands, fPOM C and N were significantly associated with root biomass (all $p < 0.002$). In the lowland, oPOM + hcOM C and N were significantly associated with all predictors except total amino sugars (all $p < 0.05$). In contrast, in the upland, oPOM + hcOM C and N were significantly associated with roots and the interaction between root quality and treatment (all $p < 0.05$). In the lowland, MAOM C was marginally related to root biomass ($p = 0.081$), but MAOM N was not related to any predictor. In contrast, in the upland, MAOM C and N were both significantly associated with the interactions of treatment and root quality and treatment and DOM C, and MAOM N was additionally related to the interaction of treatment and root biomass (all $p < 0.05$).

4. Discussion

Despite 30 years of ~30% higher average water inputs and corresponding increased plant inputs (Knapp et al., 2001; Wilcox et al., 2016), soil C and N stocks remained largely unchanged in this mesic grassland. Although lack of responsiveness of soil C and N has been reported previously (Wilcox et al., 2016), this finding is noteworthy considering the high interest in C sequestration in grasslands (Bai and Cotrufo, 2022) with the expectation that managing grasslands to increase plant production can result in increased soil C. While we found minimal influence on bulk soil C and N stocks, increased precipitation modified C and N in SOM fractions in ways that align with controls of SOM formation and loss, improving our understanding of soil biogeochemical feedbacks to climate change.

4.1. Limited responses of bulk SOM C and N

The limited response of bulk soil C and N in this study, despite previously reported changes in some key underlying processes, were likely driven by increased C and N cycling, with minimal change in stocks of C and N. This inference is supported by our findings and by previous work which suggested that greater aboveground (Wilcox et al., 2016) and belowground plant inputs (Fig. 4) combined with higher soil respiration led to balanced changes in C inputs and outputs with increased precipitation (Knapp, 1998; Broderick et al., 2022a). Prior studies in the same increased precipitation experiment also support the potential for higher N losses with greater water availability, with higher root δ^{15}N, soil ammonium concentrations, N mineralization, and nitrification reported under increased precipitation at this site, depending on landscape position (Wilcox et al., 2016; Broderick et al., 2022b). Notably, at our site, soil volumetric water content seldom exceeded 0.6 (Supplementary Fig. 1b) and microbial activity, exemplified by increased N cycling, seems to have increased, suggesting microbes were not experiencing oxygen limitation, a potential outcome of increased precipitation in mesic grasslands. Microbes were also potentially less stressed due to less inter- and intra-annual variation in added water and soil moisture in increased precipitation plots (Supplementary Fig. 1). Thus, it is likely that increased precipitation had a similar stimulatory effect on both the inputs and outputs of soil C and N, resulting in minimal change in bulk C and N pools. However, we cannot rule out that the relatively small increase in average soil moisture, although highly variable within and among years, in the increased precipitation plots (4.5%) may not have been large enough to result in strong soil responses (Supplementary Fig. 1b). Regardless, SOM fractions were more responsive than bulk soil C and N and provided mechanistic insights into soil C and N responses to increased precipitation.

4.2. Connecting SOM fraction responses to biotic drivers

Separating SOM into physical fractions is increasingly seen as a path toward better understanding of soil C and N responses to global change (Lavallee et al., 2020). Given our evolving understanding of SOM fraction formation and loss, investigating these controls in response to global changes will be key for determining the usefulness of studying physical SOM fractions empirically and the best way to formulate and parameterize these fractions in SOM models. Our hypotheses for responses of specific SOM fractions to increased precipitation were based on current dominant theories of SOM formation and loss (e.g., Cotrufo et al., 2013; Cotrufo et al., 2015; Liang et al., 2017; Sokol et al., 2019), but these had mixed support from our data.

We found increased fPOM N under increased precipitation and suggest that this was likely driven by enhanced plant inputs from increased

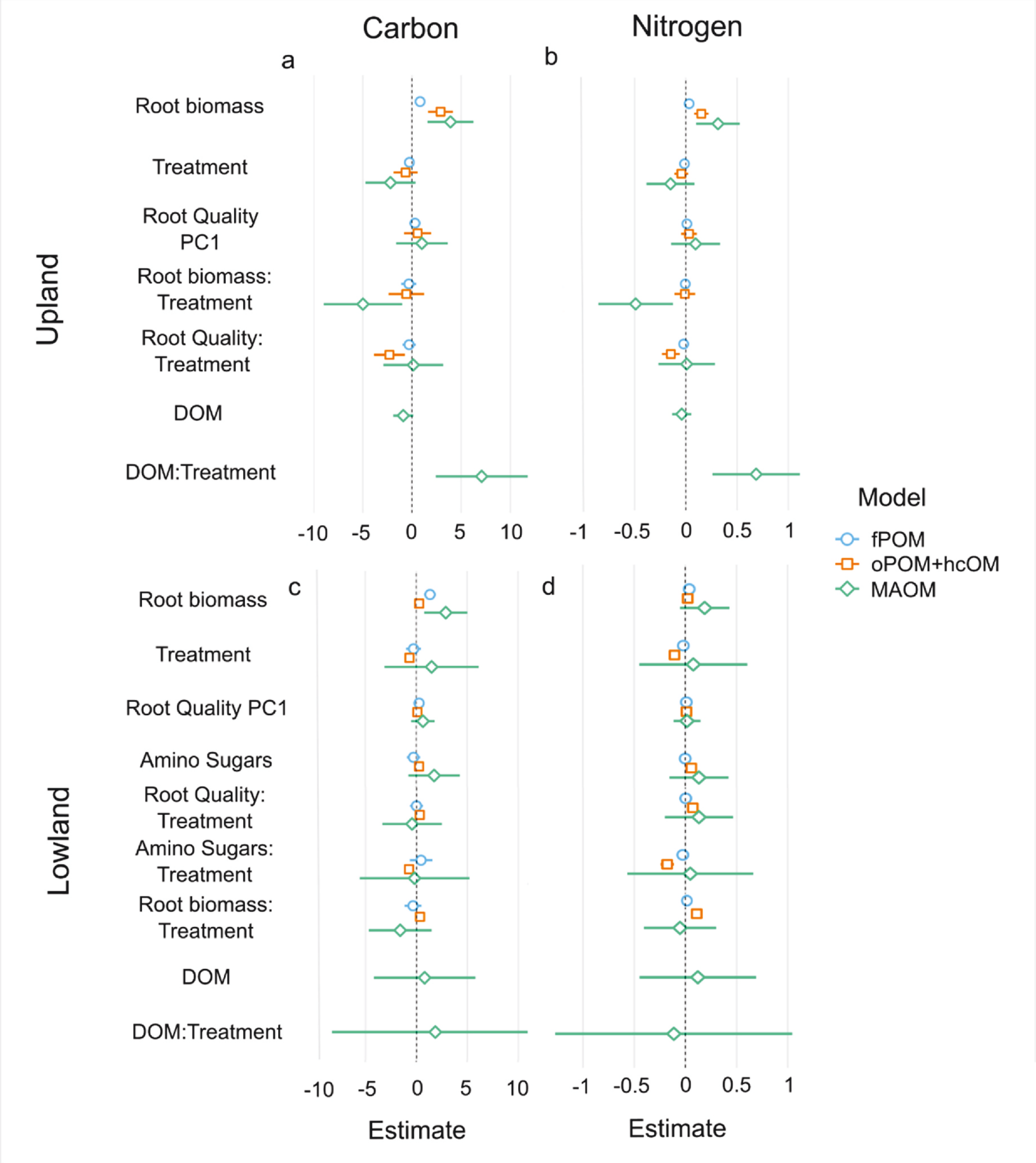

Fig. 5. Estimates of coefficients in a multiple regression model predicting free particulate organic matter (fPOM; blue), occluded POM and heavy, coarse OM (oPOM + hcOM; orange), and mineral-associated organic matter (MAOM; green) carbon (a+c) and nitrogen (b + d) at upland (a+b) and lowland (c + d) landscape positions.

root biomass under increased precipitation (Figs. 1, 4 and 5). While we expected faster N cycling under increased precipitation (Broderick et al., 2022b) to be related to increased N mineralization of fPOM that would outweigh plant N inputs and result in depletion of the fPOM fraction, our results suggest the opposite. Forb and legume biomass increased under increased precipitation (Wilcox et al., 2016), which may have promoted more structural (forb) and N-rich (legume) plant inputs that could contribute to the fPOM pool (Vázquez-de-Aldana et al., 2000; Six et al., 2001; Cotrufo et al., 2015). Notably, the association of fPOM N and root biomass adds support to the importance of root litter contributions to POM pools (Villarino et al., 2021). Root contributions to POM are particularly important in grassland ecosystems where frequent fire, an inherent ecological feature and common management practice, removes aboveground biomass (Knapp et al., 1998). While PyOM was largely unaffected by increased precipitation, contrary to our expectations, it is possible that the relatively high proportion of PyN in the soil N pool (2–18%; Fig. 3) contributed to lower N loss from fPOM than expected in an unburned grassland (Soong and Cotrufo, 2015).

While responses of fPOM N to increased precipitation occurred across topographic positions, significant responses of oPOM + hcCOM and MAOM were restricted to the lowland. These lowland-specific findings were expected based on prior results (Broderick et al. 2022a, 2022b) and align with the understanding that soil properties, in this case deeper soils with a slightly higher clay content in the lowland, interact with water availability and thus can contextualize responses to global change (Austin et al., 2004). In the lowland the oPOM + hcOM pool increased in quality (e.g., decreased C:N; Fig. 1) but not in amount in response to increased precipitation, suggesting greater aggregation is likely not the driver, as we had expected (Caplan et al., 2019). Lower oPOM + hcOM C:N was also unlikely to be driven by higher quality root inputs or greater entrapment of microbial materials or PyOM in aggregates. Rather, we found that increased precipitation decreased root input quality (e.g., increased root AUR; Fig. 4), had no effect on amino sugars (Fig. 2), and increased PyC:PyN in the lowland (Fig. 3), respectively. Carbon and N in oPOM + hcOM responded in similar direction and magnitude to plant and microbial measures when combined in multiple regression (Fig. 5), suggesting coupled C and N responses to the belowground drivers we measured. Thus, lower oPOM + hcOM C:N (i.e., an uncoupled response) under increased precipitation may instead be driven by enhanced soil N availability under increased precipitation (Broderick et al., 2022b).

In contrast to the other fractions, MAOM C and N were not significantly related to any predictor in the lowland, making it difficult to determine what drove increases in lowland MAOM C and N under increased precipitation (Fig. 5). In theory, MAOM formation could have increased through either *in vivo* or *ex vivo* pathways. We focus on changes in inputs as drivers for MAOM responses since mineral protection reduces MAOM availability for decomposition. In the lowland, increased MAOM C was marginally related to increased root biomass, which is associated with higher root exudation (Fig. 5; Eisenhauer et al., 2017). However, while it has been suggested that *in vivo* MAOM formation is promoted in the rhizosphere due to efficient microbial use of root inputs (Sokol et al., 2019), we found no changes in microbial necromass quantity that aligned with greater microbial use efficiency. Rather, higher root exudation potentially could have formed MAOM via the *ex vivo* pathway (Villarino et al., 2021). We found lower DOM C and DOM C:N with increased precipitation, across the landscape transect (Fig. 1). These relatively N-rich inputs of DOM under increased precipitation may have also formed MAOM via the *ex vivo* pathway, given greater stabilization of N-rich compounds (Possinger et al., 2020). Alternatively, greater root biomass and potentially exudation could promote formation of reactive short-range order minerals that could retain relatively more C and N in MAOM (Yu et al., 2017). We were surprised that our hypothesized microbial pathway of increased MAOM formation under increased precipitation was not supported by our data, especially since the only other study we know of that investigated microbial necromass response to increased precipitation found that it increased (Shao et al., 2018). However, we note that we did not measure other potentially important microbial parameters that might align with increased MAOM formation, such as extracellular products, microbial growth and turnover rate, substrate use efficiency, or more specific microbial community data than fungi and bacteria. These may have revealed different microbial responses to increased precipitation (Trivedi et al., 2016; Sokol et al., 2022). Further, we did not measure mineralogy, which may have been modified by precipitation to increase C and N sorption via changes in redox or pH (Doetterl et al., 2015). This could be particularly important at our site given that it lies at the interface between humid and arid conditions, known to differentially influence MAOM persistence (Heckman et al., 2023). This uncertainty highlights the need for better understanding of MAOM controls. Regardless, our findings of greater stable SOM formation under increased precipitation suggest soil C storage may act as a negative feedback to increased atmospheric CO_2 in mesic environments if precipitation increases. However, the lack of change in the total SOM pool indicates that this negative feedback may be minimal.

The stronger lowland responses in this study are similar to studies examining legacy effects of our site's enhanced precipitation treatment (Broderick et al. 2022a, 2022b). The lowlands are a depositional environment, where material eroded from the upland deposits in the lowland. Depositional settings may have inherently more stable OM than erosive landscapes, due to interactions between OM inputs and reactive minerals to form MAOM (Berhe and Kleber, 2013). The potentially higher availability of OM and reactive materials at the lowland site may facilitate the stronger responses of minerally-protected OM pools to increased precipitation in this study. However, we find that MAOM C stock is higher in the upland than the lowland in the 5–15 cm depth, suggesting greater reactive minerals and OM in the lowland may be less important for our results (Supplementary Fig. 4). Alternatively, greater rooting volume of the deeper lowland soils may have supported more root-microbe interactions that could facilitate MAOM formation (Sokol and Bradford, 2019). Additionally, the depositional setting of the lowland created deeper soils, which have higher soil water content under increased precipitation, promoting N cycling and stable SOM responses (Haddix et al., 2020; Broderick et al. 2022a, 2022b). Differences in depth between lowland soils and upland soils may be why we did not find interactions of increased precipitation treatment and soil depth at our site. The shallow upland soils prevented us from consistently sampling down to 30 cm. More studies on precipitation alteration in deeper soils will help clarify if variable responses occur over depth, as has been found for other global changes (Rocci et al., 2021; Soong et al., 2021).

4.3. Conclusions

Although bulk soil C and N were unresponsive to three decades of increased precipitation in this mesic grassland, we found differing responses of SOM fractions that could be used to evaluate dominant SOM theories. Changes in soil N availability and plant input quantity and quality under increased precipitation, that surpassed potential increases in microbial decomposition, likely drove POM pool responses. However, MAOM responses were more difficult to explain, reflecting the idea that MAOM has a diversity of inputs and controls that are not always easily or commonly measured (Rasmussen et al., 2018; Whalen et al., 2022). Determining the mechanistic controls of POM and MAOM, and how they vary with increased precipitation will be key for understanding and predicting soil biogeochemical feedbacks to climate change. Relatedly, there is strong interest in using grassland soils for C storage to mitigate climate change (Bai and Cotrufo, 2022). Our study suggests that soil C may be preferentially stored in MAOM under increased precipitation, which could promote a more resilient soil C pool to other global changes, such as warming (Rocci et al., 2021). However, relatively small responses of MAOM in this study, that do not translate to the total SOM pool, suggest that changes in the stable OM pool under increased precipitation will likely not be sufficient to provide a strong negative feedback to climate change in mesic grasslands.

Declaration of competing interest

The authors declare that they have no known competing financial interests or personal relationships that could have appeared to influence the work reported in this paper

Data availability

Data are available at: https://doi.org/10.6073/pasta/013ad4046d67f660da8e1843b2ec8c93

Acknowledgements

We thank Rebecca Even and Sam Leuthold for their assistance in the field. We thank Rainy Comley for their assistance with the pyrogenic carbon and nitrogen measurements and Mike Zhu and Carson Thompson for their assistance with the amino sugar measurements. This work was funded by a National Science Foundation Graduate Research Fellowship and Colorado State University Graduate Degree Program in Ecology small grant both awarded to K. S. Rocci. Support for the Irrigation Transect Experiment at the Konza Prairie Biological Station was provided by NSF Long-Term Ecological Research (LTER) grants to Kansas State University. Support for Chao Liang and amino sugar measurement was provided by National Natural Science Foundation of China (No. 32241037).

Appendix A. Supplementary data

Supplementary data to this article can be found online at https://doi.org/10.1016/j.soilbio.2023.109145.

References

ANKOM Technology, 2022. A200 Analytical Procedures. https://www.ankom.com/analytical-methods-support/fiber-analyzer-a200.

Austin, A.T., Yahdjian, L., Stark, J.M., Belnap, J., Porporato, A., Norton, U., Ravetta, D. A., Schaeffer, S.M., 2004. Water pulses and biogeochemical cycles in arid and semiarid ecosystems. Oecologia 141, 221–235.

Bai, T., Wang, P., Hall, S.J., Wang, F., Ye, C., Li, Z., Li, S., Zhou, L., Qiu, Y., Guo, J., 2020. Interactive global change factors mitigate soil aggregation and carbon change in a semi-arid grassland. Global Change Biology 26, 5320–5332.

Bai, W., Wan, S., Niu, S., Liu, W., Chen, Q., Wang, Q., Zhang, W., Han, X., Li, L., 2010. Increased temperature and precipitation interact to affect root production, mortality, and turnover in a temperate steppe: implications for ecosystem C cycling. Global Change Biology 16, 1306–1316.

Bai, Y., Cotrufo, M.F., 2022. Grassland soil carbon sequestration: current understanding, challenges, and solutions. Science 377, 603–608.

Berhe, A.A., Kleber, M., 2013. Erosion, deposition, and the persistence of soil organic matter: mechanistic considerations and problems with terminology. Earth Surface Processes and Landforms 38, 908–912.

Broderick, C.M., Wilkins, K., Smith, M.D., Blair, J.M., 2022a. Climate legacies determine grassland responses to future rainfall regimes. Global Change Biology 28 (8), 2639–2656.

Broderick, C.M., Freeman, K.M., Zeglin, L.H., Blair, J.M., 2022b. Climate legacy effects shape tallgrass prairie nitrogen cycling. Journal of Geophysical Research 127, 10.

Brubaker, S.C., Jones, A.J., Lewis, D.T., Frank, K., 1993. Soil properties associated with landscape position. Soil Science Society of America Journal 57, 235–239.

Caplan, J.S., Gimenez, D., Brunsell, N.A., Blair, J.M., Knapp, A.K., 2019. Decadal-scale shifts in soil hydraulic properties as induced by altered precipitation. Science Advances 5, 1–9.

Cotrufo, M.F., Wallenstein, M.D., Boot, C.M., Denef, K., Paul, E., 2013. The Microbial Efficiency-Matrix Stabilization (MEMS) framework integrates plant litter decomposition with soil organic matter stabilization: do labile plant inputs form stable soil organic matter? Global Change Biology 19, 988–995.

Cotrufo, M.F., Soong, J.L., Horton, A.J., Campbell, E.E., Haddix, M.L., Wall, D.H., Parton, W.J., 2015. Formation of soil organic matter via biochemical and physical pathways of litter mass loss. Nature Geoscience 8, 776.

Cotrufo, M.F., Lavallee, J.M., 2022. Soil Organic Matter Formation, Persistence, and Functioning: A Synthesis of Current Understanding to Inform its Conservation and Regeneration Advances in Agronomy, pp. 1–66.

Craine, J.M., Elmore, A.J., Olson, K., Tolleson, D., 2010. Climate change and cattle nutritional stress. Global Change Biology 16, 2901–2911.

Delgado-Baquerizo, M., Bissett, A., Eldridge, D.J., Maestre, F.T., He, J.Z., Wang, J.T., Hamonts, K., Liu, Y.R., Singh, B.K., Fierer, N., 2017a. Palaeoclimate explains a unique proportion of the global variation in soil bacterial communities. Nature Ecology & Evolution 1, 1339–1347.

Delgado-Baquerizo, M., Eldridge, D.J., Maestre, F.T., Karunaratne, S.B., Trivedi, P., Reich, P.B., Singh, B.K., 2017b. Climate legacies drive global soil carbon stocks in terrestrial ecosystems. Science Advances 3, e1602008.

Diao, H., Chen, X., Zhao, X., Dong, K., Wang, C., 2022. Effects of nitrogen addition and precipitation alteration on soil respiration and its components in a saline-alkaline grassland. Geoderma 406, 115541.

Doetterl, S., Stevens, A., Six, J., Merckx, R., Van Oost, K., Casanova Pinto, M., Casanova-Katny, A., Muñoz, C., Boudin, M., Zagal Venegas, E., 2015. Soil carbon storage controlled by interactions between geochemistry and climate. Nature Geoscience 8, 780–783.

Dondini, M., Martin, M., De Camillis, C., Uwizeye, A., Soussana, J.-F., Robinson, T., Steinfeld, H., 2023. Global assessment of soil carbon in grasslands – from current stock estimates to sequestration potential. In: FAO Animal Production and Health Paper No. 187. FAO, Rome. https://doi.org/10.4060/cc3981en.

Dumont, B., Andueza, D., Niderkorn, V., Lüscher, A., Porqueddu, C., Picon-Cochard, C., 2015. A meta-analysis of climate change effects on forage quality in grasslands: specificities of mountain and M editerranean areas. Grass and Forage Science 70, 239–254.

Eisenhauer, N., Lanoue, A., Strecker, T., Scheu, S., Steinauer, K., Thakur, M.P., Mommer, L., 2017. Root biomass and exudates link plant diversity with soil bacterial and fungal biomass. Scientific Reports 7, 1–8.

Ferchaud, F., Chlebowski, F., 2020. SimpleESM: R Script to Calculate Soil Organic Carbon and Nitrogen Stocks at Equivalent Soil Mass. INRAE (France), p. 7.

Haddix, M.L., Gregorich, E.G., Helgason, B.L., Janzen, H., Ellert, B.H., Cotrufo, M.F., 2020. Climate, carbon content, and soil texture control the independent formation and persistence of particulate and mineral-associated organic matter in soil. Geoderma 363, 114160.

He, N.P., Chen, Q.S., Han, X.G., Yu, G.R., Li, L.H., 2012. Warming and increased precipitation individually influence soil carbon sequestration of Inner Mongolian grasslands, China. Agriculture Ecosystems & Environment 158, 184–191.

Heckman, K., Hicks Pries, C.E., Lawrence, C.R., Rasmussen, C., Crow, S.E., Hoyt, A.M., von Fromm, S.F., Shi, Z., Stoner, S., McGrath, C., 2022. Beyond bulk: density fractions explain heterogeneity in global soil carbon abundance and persistence. Global Change Biology 28, 1178–1196.

Heckman, K.A., Possinger, A.R., Badgley, B.D., Bowman, M.M., Gallo, A.C., Hatten, J.A., Nave, L.E., SanClements, M.D., Swanston, C.W., Weiglein, T.L., 2023. Moisture-driven divergence in mineral-associated soil carbon persistence. Proceedings of the National Academy of Sciences 120, e2210044120.

Jansson, J.K., Hofmockel, K.S., 2020. Soil microbiomes and climate change. Nature Reviews Microbiology 18, 35–46.

Jing, X., Chen, X., Xiao, W., Lin, L., Wang, C., He, J.-S., Zhu, B., 2018. Soil enzymatic responses to multiple environmental drivers in the Tibetan grasslands: insights from two manipulative field experiments and a meta-analysis. Pedobiologia 71, 50–58.

Joergensen, R.G., 2018. Amino sugars as specific indices for fungal and bacterial residues in soil. Biology and Fertility of Soils 54, 559–568.

Knapp, A.K., 1998. Determinants of soil CO2 flux from a sub-humid grassland: effect of fire and fire history. Ecological Applications 8 (3), 760–770.

Knapp, A.K., Briggs, J.M., Hartnett, D.C., Collins, S.L., 1998. Grassland Dynamics: Long-Term Ecological Research in Tallgrass Prairie. Oxford University Press, New York.

Knapp, A.K., Briggs, J.M., Koelliker, J.K., 2001. Frequency and extent of water limitation to primary production in a mesic temperate grassland. Ecosystems 4, 19–28.

Knapp, A.K., Ciais, P., Smith, M.D., 2017. Reconciling inconsistencies in precipitation–productivity relationships: implications for climate change. New Phytologist 214, 41–47.

Komatsu, K.J., Avolio, M.L., Lemoine, N.P., Isbell, F., Grman, E., Houseman, G.R., Koerner, S.E., Johnson, D.S., Wilcox, K.R., Alatalo, J.M., 2019. Global change effects on plant communities are magnified by time and the number of global change factors imposed. Proceedings of the National Academy of Sciences 116, 17867–17873.

Korell, L., Auge, H., Chase, J.M., Harpole, W.S., Knight, T.M., 2021. Responses of plant diversity to precipitation change are strongest at local spatial scales and in drylands. Nature Communications 12, 1–7.

Lajtha, K., Townsend, K.L., Kramer, M.G., Swanston, C., Bowden, R.D., Nadelhoffer, K., 2014. Changes to particulate versus mineral-associated soil carbon after 50 years of litter manipulation in forest and prairie experimental ecosystems. Biogeochemistry 119, 341–360.

Lavallee, J., Soong, J., Cotrufo, M.F., 2020. Conceptualizing soil organic matter into particulate and mineral-associated forms to address global change in the 21st century. Global Change Biology 26, 261–273.

Lee, J.-Y., Marotzke, J., Bala, G., Cao, L., Corti, S., Dunne, J.P., Engelbrecht, F., Fischer, E., Fyfe, J.C., Jones, C., 2021. Future Global Climate: Scenario-Based Projections and Near-Term Information. IPCC.

Leuthold, S.J., Haddix, M.L., Lavallee, J.M., Cotrufo, F.M., 2022. Physical Fractionation Techniques. Encyclopedia of Soils in the Environment, second ed. https://doi.org/10.1016/B978-0-12-822974-3.00067-7

Liang, C., Schimel, J.P., Jastrow, J.D., 2017. The importance of anabolism in microbial control over soil carbon storage. Nature Microbiology 2.

Liang, C., Amelung, W., Lehmann, J., Kästner, M., 2019. Quantitative assessment of microbial necromass contribution to soil organic matter. Global Change Biology 25, 3578–3590.

Liu, L., Wang, X., Lajeunesse, M.J., Miao, G., Piao, S., Wan, S., Wu, Y., Wang, Z., Yang, S., Li, P., 2016. A cross-biome synthesis of soil respiration and its determinants under simulated precipitation changes. Global Change Biology 22, 1394–1405.

McBeath, A.V., Wurster, C.M., Bird, M.I., 2015. Influence of feedstock properties and pyrolysis conditions on biochar carbon stability as determined by hydrogen pyrolysis. Biomass and Bioenergy 73, 155–173.

Moinet, G.Y.K., Cieraad, E., Hunt, J.E., Fraser, A., Turnbull, M.H., Whitehead, D., 2016. Soil heterotrophic respiration is insensitive to changes in soil water content but related to microbial access to organic matter. Geoderma 274, 68–78.

Moore, T., 2023. AET01 Konza prairie grass reference evapotranspiration. Environmental Data Initiative. https://doi.org/10.6073/pasta/b5a57131dc37d035b7c14ec7a8a49604.

Mosier, S., Apfelbaum, S., Byck, P., Calderon, F., Teague, R., Thompson, R., Cotrufo, M. F., 2021. Adaptive multi-paddock grazing enhances soil carbon and nitrogen stocks and stabilization through mineral association in southeastern US grazing lands. Journal of Environmental Management 288, 112409.

Ochoa-Hueso, R., Arca, V., Delgado-Baquerizo, M., Hamonts, K., Piñeiro, J., Serrano-Grijalva, L., Shawyer, J., Power, S.A., 2020. Links between soil microbial communities, functioning, and plant nutrition under altered rainfall in Australian grassland. Ecological Monographs 90, e01424.

Possinger, A.R., Zachman, M.J., Enders, A., Levin, B.D., Muller, D.A., Kourkoutis, L.F., Lehmann, J., 2020. Organo–organic and organo–mineral interfaces in soil at the nanometer scale. Nature Communications 11, 1–11.

R Core Team, 2019. R: A Language and Environment for Statistical Computing. R Foundation for Statistical Computing Vienna, Austria.

Ren, C., Zhao, F., Shi, Z., Chen, J., Han, X., Yang, G., Feng, Y., Ren, G., 2017. Differential responses of soil microbial biomass and carbon-degrading enzyme activities to altered precipitation. Soil Biology and Biochemistry 115, 1–10.

Reynolds, S.G., 2005. In: Suttie, J.M., Reynolds, S.G., Batello, C. (Eds.), Introduction, Grasslands of the World. Food and Agricultural Organization of the United Nations, Rome.

Rocci, K.S., Lavallee, J.M., Stewart, C.E., Cotrufo, M.F., 2021. Soil organic carbon response to global environmental change depends on its distribution between mineral-associated and particulate organic matter: a meta-analysis. Science of the Total Environment 793. https://doi.org/10.1016/j.scitotenv.2021.148569.

Sala, O.E., Parton, W.J., Joyce, L., Lauenroth, W., 1988. Primary production of the central grassland region of the United States. Ecology 69, 40–45.

Shao, P., He, H., Zhang, X., Xie, H., Bao, X., Liang, C., 2018. Responses of microbial residues to simulated climate change in a semiarid grassland. Science of the Total Environment 644, 1286–1291.

Six, J., Guggenberger, G., Paustian, K., Haumaier, L., Elliott, E.T., Zech, W., 2001. Sources and composition of soil organic matter fractions between and within soil aggregates. European Journal of Soil Science 52, 607–618.

Sokol, N.W., Bradford, M.A., 2019. Microbial formation of stable soil carbon is more efficient from belowground than aboveground input. Nature Geoscience 12, 46–53.

Sokol, N.W., Sanderman, J., Bradford, M.A., 2019. Pathways of mineral-associated soil organic matter formation: integrating the role of plant carbon source, chemistry, and point of entry. Global Change Biology 25, 12–24.

Sokol, N.W., Whalen, E.D., Jilling, A., Kallenbach, C., Pett-Ridge, J., Georgiou, K., 2022. The global distribution, formation, and fate of mineral-associated soil organic matter under a changing climate–A trait-based perspective. Functional Ecology 36 (6), 1411–1429.

Soong, J.L., Castanha, C., Pries, C.E.H., Ofiti, N., Porras, R.C., Riley, W.J., Schmidt, M.W., Torn, M.S., 2021. Five years of whole-soil warming led to loss of subsoil carbon stocks and increased CO2 efflux. Science Advances 7, eabd1343.

Soong, J.L., Parton, W.J., Calderon, F., Campbell, E.E., Cotrufo, M.F., 2015. A new conceptual model on the fate and controls of fresh and pyrolized plant litter decomposition. Biogeochemistry 124, 27–44.

Soong, J.L., Cotrufo, M.F., 2015. Annual burning of a tallgrass prairie inhibits C and N cycling in soil, increasing recalcitrant pyrogenic organic matter storage while reducing N availability. Global Change Biology 21, 2321–2333.

Staub, B., Rosenzweig, C., 1992. Global Zobler Soil Type, Soil Texture, Surface Slope, and Other Properties, Digital Raster Data on a 1-degree Geographic (Lat/long) 180X360 Grid, Global Ecosystems Database Version 2.0. Seven Independent Spatial Layers, 561,782 Bytes in 16 Files. NOAA National Geophysical Data Center, Boulder, CO.

Tappi, 1981. Water Solubility of Wood and Pulp. Test Method T204 (Or 207). Technical Association of the Pulp and Paper Industry, Atlanta.

Trivedi, P., Delgado-Baquerizo, M., Trivedi, C., Hu, H., Anderson, I.C., Jeffries, T.C., Zhou, J., Singh, B.K., 2016. Microbial regulation of the soil carbon cycle: evidence from gene–enzyme relationships. The ISME Journal 10, 2593–2604.

Vázquez-de-Aldana, B.R., Pérez-Corona, M.E., García-Criado, B., 2000. Nutritional quality of semi-arid grassland in western Spain over a 10-year period: changes in chemical composition of grasses, legumes and forbs. Grass and Forage Science 55, 209–220.

Villarino, S.H., Pinto, P., Jackson, R.B., Piñeiro, G., 2021. Plant rhizodeposition: a key factor for soil organic matter formation in stable fractions. Science Advances 7, eabd3176.

Vilonen, L.L., Blair, J., Trivedi, P., Zeglin, L., Smith, M.D., 2022. Limited legacy effects of extreme multiyear drought on carbon and nitrogen cycling in a mesic grassland. Elem Sci Anth 10, 000093.

Wang, B., Chen, Y., Li, Y., Zhang, H., Yue, K., Wang, X., Ma, Y., Chen, J., Sun, M., Chen, Z., 2021. Differential effects of altered precipitation regimes on soil carbon cycles in arid versus humid terrestrial ecosystems. Global Change Biology 27, 6348–6362.

Wang, P., Huang, K., Hu, S., 2020. Distinct fine-root responses to precipitation changes in herbaceous and woody plants: a meta-analysis. New Phytologist 225, 1491–1499.

White, R., Murray, S., Rohweder, M., 2000. Pilot Analysis of Global Ecosystems: Grassland Ecosystems. World Resources Institute, Washington D.C.

Wilcox, K.R., Blair, J.M., Knapp, A.K., 2016. Stability of grassland soil C and N pools despite 25 years of an extreme climatic and disturbance regime. Journal of Geophysical Research Biogeosciences 121, 1934–1945.

Wu, Q., Yue, K., Ma, Y., Heděnec, P., Cai, Y., Chen, J., Zhang, H., Shao, J., Chang, S.X., Li, Y., 2022. Contrasting effects of altered precipitation regimes on soil nitrogen cycling at the global scale. Global Change Biology 28 (22), 6679–6695.

Wurster, C.M., Lloyd, J., Goodrick, I., Saiz, G., Bird, M.I., 2012. Quantifying the abundance and stable isotope composition of pyrogenic carbon using hydrogen pyrolysis. Rapid Communications in Mass Spectrometry 26, 2690–2696.

Yang, Z., Wei, Y., Fu, G., Song, H., Li, G., Xiao, R., 2020. Asymmetric effect of increased and decreased precipitation in different periods on soil and heterotrophic respiration in a semiarid grassland. Agricultural and Forest Meteorology 291, 108039.

Yue, K., Fornara, D.A., Yang, W., Peng, Y., Peng, C., Liu, Z., Wu, F., 2017. Influence of multiple global change drivers on terrestrial carbon storage: additive effects are common. Ecology Letters 20, 663–672.

Yue, K., Jarvie, S., Senior, A.M., Van Meerbeek, K., Peng, Y., Ni, X., Wu, F., Svenning, J. C., 2020. Changes in plant diversity and its relationship with productivity in response to nitrogen addition, warming and increased rainfall. Oikos 129, 939–952.

Zhang, X., Amelung, W., 1996. Gas chromatographic determination of muramic acid, glucosamine, mannosamine, and galactosamine in soils. Soil Biology and Biochemistry 28, 1201–1206.

Zhang, J., Ru, J., Song, J., Li, H., Li, X., Ma, Y., Li, Z., Hao, Y., Chi, Z., Hui, D., 2022. Increased precipitation and nitrogen addition accelerate the temporal increase of soil respiration during eight-year old-field grassland succession. Global Change Biology 28 (12), 3944–3959.

Zuur, A.F., Ieno, E.N., Elphick, C.S., 2010. A protocol for data exploration to avoid common statistical problems. Methods in Ecology and Evolution 1, 3–14.